International Journal for Housing Science and Its Applications
Publish August 6, 2025. Volume 46, Issue 3 Pages 8398-8406

https,//doi.org/10.70517/ijhsa463718

Multi-scenario analysis and simulation of global traffic accidents based on UAV 3D reconstruction technology

Huawei Xie[1,2,*], Weijun Li[1,2], Jinzhou Su[1,2] and Shuliang Tu[3]
[1] Department of Forensic Science, Fujian Police College, Fuzhou, Fujian, 350007, China
[2] The Engineering Research Center, Fujian Police College, Fuzhou, Fujian, 350007, China
[3] Longyan Public Security Bureau, Longyan, Fujian, 364000, China
Corresponding authors: (e-mail: xiehuawei.fjpsc@vip.163.com).

Abstract UAV 3D reconstruction technology provides explorable new ways to digitize traffic accident scenes. In this paper, a parallelized incremental UAV image 3D reconstruction algorithm (SFM) is proposed. Combining vocabulary tree retrieval and GPS constraints to optimize beam method leveling (BA), it significantly improves the reconstruction accuracy and speed of the accident scene. A traffic accident simulation system based on virtual reality technology is designed to realize pre-collision, post-collision, and initial speed inversion and multi-morphology accident simulation. The results show that: in the multi-group ranging experiments, the absolute error value of UAV ranging in this paper is 0.22 at maximum, and the relative error is only 0.43% at maximum, which is smaller than 5.30 and 8.76% of the traditional method. Combined with the image of 4.5m+25m aerial height to complete the modeling, the absolute error in x and y direction is only 0.00m and 0.58m, and the relative error is 0.125 and 0.250. Using the model to restore the situation at the time of the accident, the change of acceleration at the time of the three head injuries can be accurately calculated.

Index Terms three-dimensional reconstruction, parallelized incremental SFM, vocabulary tree retrieval, GPS constraints, beam method leveling, traffic accident simulation

I. Introduction

Road traffic accident scene usually left a large number of objective traces of physical evidence related to the accident, is to analyze the causes of traffic accidents, determine the basis of the responsibility for the accident, but also may be the source of evidence material for judicial arbitration, insurance claims [1]. Such as the accident scene ground traces and scattered objects can be used as the basis for inferring the location of the collision, the vehicle involved in the incident when the emergency braking in the scene left brake marks can be used to calculate the vehicle in the starting point of the braking traces of the driving speed, etc. [2]-[4]. Road traffic accident scene fast processing, is conducive to the incident section of the traffic congestion as soon as possible to ease, reduce the long time scene investigation process may be the security risk of secondary accidents [5].

At present, China's traffic accident scene investigation mainly relies on the camera photo fixation, ruler measurement, hand-drawn site map and other two-dimensional means of investigation, for some key traces of physical evidence of the photo fixation, positioning and measurement and other necessary work, often need to invest the necessary manpower, time, it is difficult to do rapid processing, resulting in traffic congestion continues to worsen [6]-[8]. For large-scale traffic accidents, especially when occurring on the highway, two-dimensional investigation means appear to be insufficient, in order to obtain more comprehensive accident information, can only prolong the scene investigation time, occupy the accident section, and even interrupt traffic, very easy to cause secondary traffic accidents [9]-[11]. In addition, large-scale accident investigation is prone to site information leakage, inaccurate survey measurement dimensions and other difficult to re-survey the situation, affecting the subsequent identification of accidents, cause analysis, responsibility determination, etc. [12]. Therefore, there is an urgent need to improve the means of road traffic accident scene investigation.

Image-based 3D reconstruction can accurately recover the geometry of the real scene from a set of two-dimensional multi-view images, which has important theoretical research significance and application value [13]. In recent years, the functions of consumer-grade UAVs have been enhanced and increased, and users can use UAVs to obtain high-resolution image sequences with position information, which makes the image-based 3D reconstruction of the scene optimized [14], [15]. Literature [16] explored the use of UAVs to reconstruct accident scenes, testing the impact of flight parameters such as heading angle and waypoint, on the reconstruction of traffic accident scenes to achieve centimeter-level reconstruction accuracy. Literature [17] utilized low-cost UAVs and structured light measurements to analyze and simulate traffic accidents, which is more accurate, efficient, and

capable of generating a scene model with accurate measurement data and reusability compared to traditional methods. Literature [18] proposed a digital reconstruction of road traffic accidents using a low-cost, miniaturized and lightweight unmanned aerial vehicle (UAV), which was tested in a variety of scenarios and achieved good practical results. Literature [19] proposed a method to efficiently reconstruct a traffic accident scene based on UAV stereo photogrammetry (UAV-SfM) and Global Positioning System (GNSS) equipment. Literature [20] uses a laser scanner (TLS) and unmanned aerial vehicle (UAV) technology complex traffic accident scene for measurement and modeling, which obtains orthophotos from UAV photographs and point clouds, and the relative error of this method is controlled within 6 cm compared with the actual police measurements.

Comprehensively, the above literature shows that UAV aerial photography technology has obvious advantages in traffic management and traffic accident scene investigation [21]. However, the technology in the accident scene investigation work only stays in the two-dimensional level such as photo and video, and there are certain limitations in the presentation of scene information [22], [23]. For example, the three-dimensional correlation between the scene traces and the road environment is insufficient, and the correlation between the three-dimensional scene of the incident and the cause of the accident is missing [24]. The information presented by the real-life 3D reconstruction can not only avoid the above limitations, but also be more three-dimensional and objective in the presentation of the three-dimensional relative positional relationship between the accident participants and the road environment [25].

There are limitations such as low efficiency, error accumulation and scene drift in general large-scale UAV road image 3D reconstruction. To address the problems, this paper reduces the complexity of image feature matching through the vocabulary tree retrieval and scene graph division strategies, and optimizes the incremental SFM algorithm by combining multi-core parallel computing. The beam method leveling algorithm with GPS constraints is introduced to suppress error accumulation and scene drift. A three-layer virtual reality simulation system is constructed, integrating geometric modeling, dynamics analysis and visualization modules to complete multi-scene collision dynamics modeling and velocity inversion analysis. Through the accident simulation experiment, it is proved that the method of this paper can accurately restore the specific situation of the accident.

II. Realization of traffic accident simulation based on UAV three-dimensional reconstruction technology

II. A. Specific process for 3D reconstruction of parallelized UAV imagery

The incremental SFM reconstruction algorithm is robust to outliers and can be used for sparse reconstruction of UAV images. However, the incremental SFM reconstruction algorithm still suffers from the following problems when dealing with large-scale UAV highway datasets: on the one hand, in order to construct stable geometric constraints, the UAV needs to acquire a large number of multiview images and configure a high overlap between the heading and the sideways trajectory, which leads to a higher complexity of the image search for matching pairs. The combination complexity becomes higher and the efficiency of feature matching decreases. On the other hand, the efficiency of BA optimization decreases significantly with the increase of the number of images because BA optimization is performed iteratively with newly registered images. In addition, due to the influence of the errors of the previous feature matching tasks, each iteration of BA optimization will generate new errors, and eventually the global BA optimization may not be able to be carried out due to the accumulation of too large an error, leading to the final results of the scene drifting phenomenon. Aiming at the above problems, this paper proposes a 3D reconstruction algorithm for UAV images that can be parallelized.

Figure 1 shows the specific process of the algorithm. Different from the original incremental SFM reconstruction algorithm, before feature matching, this paper uses the lexical tree image retrieval technology to select the relevant image set for each image to be matched, so as to avoid feature matching calculation with some images with low or even unrelated correlation, reduce the combination complexity of matching pairs, and improve the matching efficiency. Then, a weighted scene graph is constructed based on the vocabulary tree retrieval by considering the number of feature matches and the GPS information provided by the UAV platform, and the scene graph is partitioned and extended, after which each partitioned subset is distributed on a multi-core CPU to execute incremental SFM in parallel. This not only makes full use of the computational resources, but also the optimization parameters of the beam method leveling step are significantly reduced with the decrease of image size, thus accelerating the reconstruction process. Finally, the reconstruction results of each subset are merged based on the common reconstruction points among the subsets. Since the reconstructed individual scenes have different errors, the algorithm performs global beam method leveling to optimize the merged overall model, in addition, in order to avoid scene drift, this paper combines the GPS information to add a position constraint term for the beam method leveling cost function. Finally, the generated sparse point cloud is used as the seed surface element, and the

reconstruction and filtering of surface elements are performed iteratively to obtain the dense point cloud model of the real highway scene.

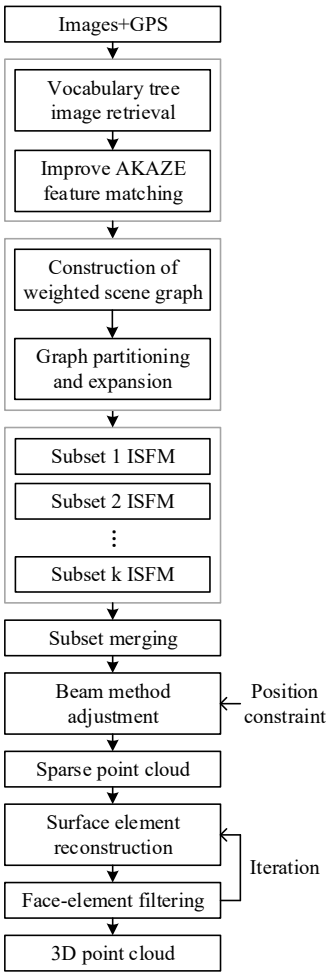

Figure 1: The specific process of the algorithm

II. A. 1) Scene graph segmentation and parallel reconstruction

After the scene graph is constructed, this paper chooses the normalized cut (Ncut) algorithm to divide the scene graph, and proposes two constraints to constrain the division process: the size constraint and the completeness constraint, the size constraint gives the upper bound of the images in each subset, and the completeness constraint is defined as $\eta_{(i)} = \frac{\sum_{j \neq i} | C_i \cap C_j |}{C_i}$, where C_i and C_j represent the subsets i and j, respectively, which ensures that there are enough common images among the subsets to be merged reliably. The normalized cut algorithm is easy to cut edges with small weights to generate subsets with compact internal connections. Define the scene graph as $G = (V, E)$, where V represents vertices and E represents edges. Assuming that the scene graph needs to be partitioned into two disjoint subsets A and B, the normalized cut can be represented as

$$Ncut = (A,B) = \frac{cut(A,B)}{assoc(A,V)} + \frac{cut(A,B)}{assoc(B,V)} \tag{1}$$

where $cut = (A,B)$ is the sum of weights of all connected edges of subset A and subset B, and $assoc(A,V) = \sum_{u \in A, t \in V} w(u,t)$ denotes the correlation between the points in subset A and all other points in the scene

graph, and $assoc(B,V)$ has the same definition. After the scene graph is divided, each image is assigned to only one subset.

II. A. 2) GPS information assisted beam method leveling

Beam method leveling achieves the purpose of optimizing the recovered camera position and 3D spatial point coordinates by minimizing the reprojection error. However, due to the characteristics of the large-scale images captured by the UAV and the errors brought by the feature matching step in the early stage, new errors will be introduced in each iteration of the beam method of parallax execution, in which case, if we rely on the minimization of the reprojection error alone, the cost function of the beam method of parallax will not be able to converge to the global minimum due to the accumulation of too much error, which will lead to the final result of the scene drifting. In order to avoid scene drift, this paper combines the GPS information acquired by the UAV platform with the beam method of leveling, and adds new constraints to the cost function of the beam method of leveling, i.e., the absolute GPS error is introduced, and at the same time, the image reprojection error and the camera center distance error are reduced, so as to obtain the optimal three-dimensional spatial coordinates of the points and the camera pose that satisfy the visual constraints and position constraints at the same time, and the cost function of the beam method of leveling is the same as the GPS absolute error. The cost function is a linear combination of the GPS absolute error and the minimized reprojection error, which is achieved by minimizing the beam method leveling cost function.The representation of the GPS absolute error term is shown in Equation (2):

$$E_{gps} = \sum_{i=1}^{n} \vartheta * Huber(C_i - P_i^{gps}) \tag{2}$$

The cost function after adding equation (2) is as follows:

$$E(C,X) = \sum_{i=1}^{n}\sum_{j=1}^{m} \rho_{ij} \parallel p(C_j, X_i) - x_{ij} \parallel^2 + \sum_{i=1}^{n} \vartheta * Huber(C_i - P_i^{gps}) \tag{3}$$

The first term in Equation (3) is denoted as the reprojection error, which represents the visual constraint relationship. The second term is the absolute GPS error, which represents the positional constraints, where ϑ is the compensation coefficient, c_i denotes the predicted position of camera i, P_i^{sps} denotes the actual corresponding GPS position of the camera, and $Huber(C_i - P_i^{gps})$ is the Huber loss function of the difference between the two. The Huber loss function, which is a smooth loss function that maintains good performance despite the presence of outliers, is the difference between the two. The introduction of the absolute GPS error limits the position of the predicted camera center point, i.e., constrains the camera motion trajectory, which makes it possible to reduce the distance between the predicted camera motion trajectory and the real GPS trajectory with the continuous addition of images in the process of incremental reconstruction, which effectively eliminates the cumulative error and avoids the appearance of the scene drifting phenomenon.

II. B.Analog system design

II. B. 1) Overall structural design

Under the virtual reality technology, the design and development of traffic accident simulation system, the system can be divided into three layers of structure. Figure 2 shows the system structure.

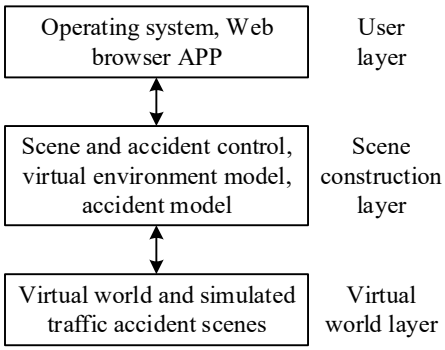

Figure 2: System structure

For the traffic accident simulation system in this design, the content of the three-layer structure in the system is different.

User layer: mainly is the user's actual operation and application aspects, to have good human-computer interaction, can be through the operating system, Web browser, APP interaction, to realize the user's operability of the virtual object.

Scene construction layer: collect relevant text, maps, data, pictures, sounds, videos, photos, etc., and be able to predefine different virtual scene models based on geometric models as well as image modeling techniques, and construct the internal resource allocation environment of the system.

Virtual World Layer: Call the scene model, correct the model based on the effective data provided by on-site investigation and eyewitnesses, and virtualize the traffic accident scene.

II. B. 2) Modeling of the virtual environment

In the design of traffic accident simulation system, the application of virtual reality technology, based on the common scene of traffic accidents to build three-dimensional models, the application of texture mapping, rendering simulation simulation of a high sense of realism of the virtual reality three-dimensional realm module resources, deposited into the system scene construction layer for users to build the later accident scene scene directly call, for the rapid restoration of the scene of the accident scene to provide a powerful help.

II. B. 3) Accident modeling

System development programming technicians to use the relevant procedures, set up on traffic accidents, “collision, roll, burning, explosion and heat wave airflow” of the special effects, and can be applied to the programming function VegaAPI control the accident time, collision intensity, roll height distance, flying out of the direction and so on.

II. C.Incident modeling applications

II. C. 1) Post-impact velocity simulation calculation

The post-collision trajectory model is called for simulation calculation. The velocity and angular velocity of the accidental vehicle in the ground coordinate system at the instant after the collision effect as the initial value of the vehicle's motion simulation after the collision effect can be obtained from the following relationship according to the vehicle's collision and stopping position as well as the direction angle by using the direct search method in the optimization method:

$$X_{ik} = f_{xi}(V_{xi}, V_{yi}, \omega_i) \tag{4}$$

$$Y_{ik} = f_{yi}(V_{xi}, V_{yi}, \omega_i) \tag{5}$$

$$\theta_{ik} = f_{\theta i}(V_{xi}, V_{yi}, \omega_i) \tag{6}$$

$$| X_{ik} - X_i | < \delta_x \tag{7}$$

$$| Y_{ik} - Y_i | < \delta_y \tag{8}$$

$$| \theta_{ik} - \theta_i | < \delta_\theta \tag{9}$$

where $X_{ik}, Y_{ik}, \theta_{ik}$ are the coordinates of the stopping position of the colliding vehicle and the direction angle of the front end obtained from the simulation, and X_i, Y_i, θ_i are the coordinates of the stopping position of the actual vehicle and the direction angle. δ_x, δ_y and δ_θ are the set error ranges. From the trajectory model, the motion of the vehicle after the collision can be simulated by the velocity angular velocity at the instant after the collision according to the principle of dynamics, and f_{xi}, f_{yi} and $f_{\theta i}$ are its abstract expressions. And the optimized values of instantaneous velocity and angular velocity after touching can be found by using the direct search method such as Fibonacci's method or the golden section method for solving the extremum problems of unconstrained nonlinear functions.

II. C. 2) Simulation calculation of pre-impact velocity

The pre-collision speed simulation calculation part calculates the speed of the accident vehicle at the instant before the collision by calling the appropriate collision model according to the obtained instantaneous speed after the collision. The system is internally set up with 80 kinds of accident patterns, and there are several solution methods for each kind of accident pattern of the collision model. The system automatically selects the best solution method

to solve the pre-collision speed and angular velocity based on the field information. As an alternative, an interface to regulate the selection of solution methods is also provided to compare different solution methods.

Figure 3 shows the structure of the pre-collision velocity simulation calculation. For example, for the accident type of a general oblique collision between a car and the side of a car, the collision model provides a momentum method, a momentum and center of contact method, a momentum-energy method, an integrated method, and so on. Different solution methods correspond to different input field information, and the system automatically searches for the best solution method to solve under the specific field input information.

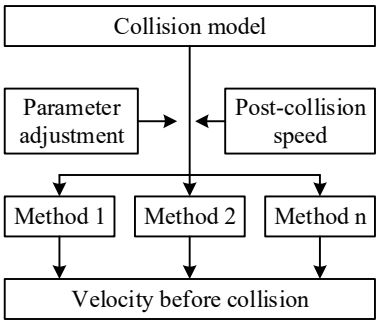

Figure 3: Simulation calculation of the velocity before the collision

II. C. 3) Initial velocity simulation calculations

This part is similar to the calculation part of the post-collision velocity simulation, the difference is that the trajectory model simulation is simulated from the initial position to the position at the time of collision, and the position direction angle obtained from the vehicle simulation is a function of the initial velocity, angular velocity, and it is necessary to add the following constraints:

$$|V_{xik} - V_{xip}| < \delta_{vx} \tag{10}$$

$$|V_{yik} - V_{yip}| < \delta_{vy} \tag{11}$$

$$|\omega_{ik} - \omega_{ip}| < \delta_{\omega} \tag{12}$$

where V_{xik}, V_{yik} and ω_{ik} are the simulated velocity angular velocities at the time of the collision, and V_{xip}, V_{yip} and ω_{ip} are the pre-collision velocity angular velocities calculated by the collision model. The δ_{vx}, δ_{vy} and δ_{ω} are set error margins. These three constraints are often tested at the end. The simulation calculation of the initial velocity incorporates the driver's maneuvering actions, as manifested by the increase in trajectory curvature and the increase in angular velocity.

III. Traffic accident simulation experiment based on three-dimensional reconstruction technology

III. A. UAV field measurement experiment

III. A. 1) Results of drone field measurements

The accurate establishment of the traffic accident model, in addition to relying on the accurate design of the reconstruction technology, also requires the accurate measurement of the accident scene by the UAV. In this paper, six points A, B, C, D, E and F are taken in front of a calibrated object at a traffic accident scene, and the UAV is used to complete the image ranging related experiments to determine the accuracy of the images taken by the UAV. Table 1 shows the field measurement results of the line segments between the points. The experimental data show that the measurement error of line segment CD is the largest, bit 1.55%, and the relative errors of line segments AB, CE, DE, and EF are 0.42%, 0.29%, 0.54%, and 0.81%, respectively, which are not more than 1.00%. Overall, the relative measurement error of each line segment does not exceed 2.00%, which meets the requirements of 3D model reconstruction.

III. A. 2) Comparison of different image ranging methods

Through multiple sets of ranging experiments, the ranging accuracy of the UAV image measurement method in this paper is compared with the traditional ranging method based on Harris operator and Tsai two-step calibration method. Table 2 shows the analysis of the comparison results. In the four groups of experimental cases, the absolute error value of ranging of the traditional method reaches 5.30 at the maximum, the relative error is 8.76% at the

maximum, and the minimum is 2.11%. In contrast, this paper uses UAV for accident scene image ranging, the absolute error value is only 0.22 at maximum, the relative error is no more than 0.43% at maximum, and the minimum is only 0.07%. The accuracy of the ranging error of this paper's method is much higher than that of the traditional ranging method, and the use of UAV for accident scene image shooting can obtain accurate images required for modeling.

Table 1: On-site measurement result

	Ranging result (cm)	Actual result (cm)	Absolute error	Relative error (%)
AB	35.35	35.50	0.15	0.42
CD	34.95	35.50	0.55	1.55
CE	27.72	27.80	0.08	0.29
DE	27.65	27.80	0.15	0.54
EF	18.35	18.50	0.15	0.81

Table 2: Comparison result

Method	Ranging result (cm)	Actual result (cm)	Absolute error	Relative error (%)
Traditional method	27.75	30.50	2.75	8.76
	44.35	45.30	0.95	2.11
	48.19	50.60	2.41	4.76
	60.50	65.80	5.30	8.03
Article method	30.40	30.50	0.10	0.33
	45.27	45.30	0.03	0.07
	50.38	50.60	0.22	0.43
	65.65	65.80	0.15	0.23

III. B. Analysis of reconstruction effect

Comprehensive application of the algorithms proposed in this paper to complete the reconstruction of the traffic accident model. In the results of this test, the reconstruction results corresponding to the photos taken at different aerial heights can be used to measure the distance between any two points and the area of the plane surrounded by any multiple line segments. In order to judge the reconstruction effect of the accident model, the reconstruction measurements in the x and y directions of the model were compared and analyzed. Figure 4 shows the results of the comparison between the reconstruction measurements in the x and y directions and the reference values. Figure 5 shows the relative error distribution of the reconstructed measured dimensions in the x and y directions. The reconstructed measurements in the x and y directions at 4.5m + 25m aerial heights have the smallest error from the reference value, 0.00m and 0.58m, respectively. Meanwhile, the relative errors of reconstructed measured dimensions in x and y directions at 4.5m+25m aerial heights were also minimized. The relative error in the x-direction does not exceed 0.125 and the relative error in the y-direction does not exceed 0.250 for 30m and 20m measurement point spacing. The combined 4.5m and 25m aerial height images have a smaller error than considering only the 4.5m and 25m aerial height images. It shows that the 3D accident model reconstruction by combining the 4.5m height and 25m aerial height images in this paper can more accurately restore each scene of the accident scene.

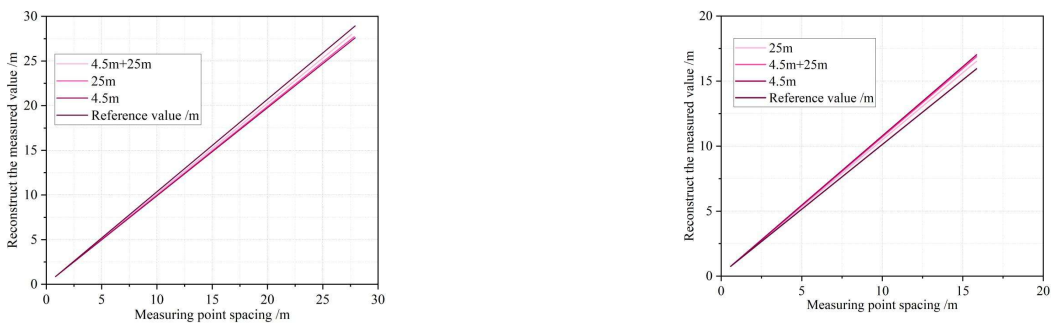

(a) X direction (b) Y direction

Figure 4: Comparison of reconstructed measured values with reference values

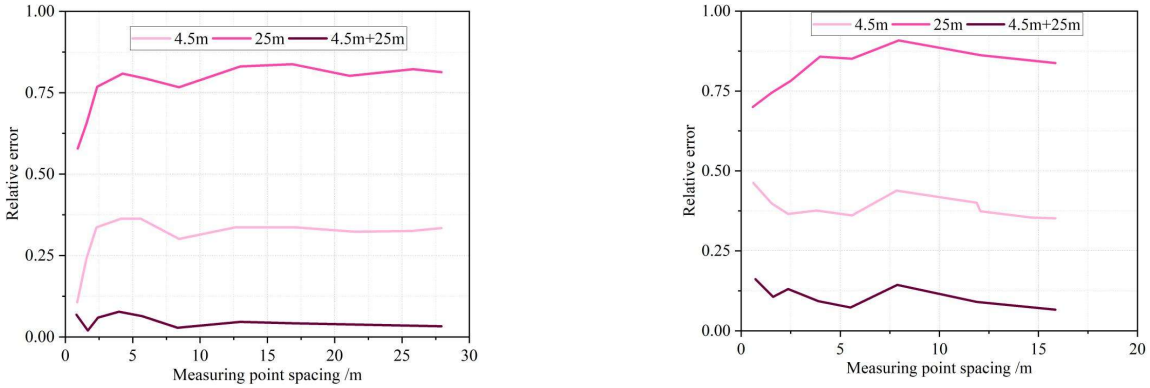

(a) X direction (b) Y direction

Figure 5: Relative error distribution of reconstructed measurements

III. C. Accident simulation effect

According to the established traffic accident model, we calculate the change of vehicle traveling speed when the accident occurs, simulate the accident process, and find the cause of the driver's injury. From the accident simulation process, it can be obtained that the motorcycle driver's head hit the ground three times, which is the direct cause of craniocerebral injury. Figure 6 shows the injury-causing forces at different time periods. Figure 6(a) shows the reduced head acceleration situation. At 450ms, the head contacted the ground for the first time, at which time the maximum peak acceleration was 448m/s2; the second contacted the ground at 698ms, at which time the head acceleration was 391m/s2, and the third contacted the ground at 950ms, at which time the head acceleration was 153m/s2.Figure 6(b) shows the acceleration of the chest. The chest also has three acceleration peaks, the maximum peak occurs at 445ms, when the chest acceleration is 340m/s2, the second peak occurs at 672ms, when the chest acceleration is 149m/s2 (the peak at 701ms is generated by the shock after the chest makes contact with the ground for the second time), and the third peak occurs at 837ms, when the chest acceleration is 97.0m/s2.The above acceleration changes can be seen in Figure 6(b), which shows the acceleration of the chest. the above acceleration changes, it can be seen that the acceleration of the head and chest basically coincide with each other, which is related to the collision of the head and chest with the ground three times during the collision movement. The first peak value of both of them appeared around 450ms, and the head and chest collided with the ground at the same time, while the chest preceded the head in the second and third times, which made the way and process of injury clear. By reconstructing the three-dimensional accident model of the UAV in the simulation system, it can meet the needs of the relevant staff to restore the accident scene, analyze the cause of the accident and the process of injury, and improve the time efficiency of accident processing.

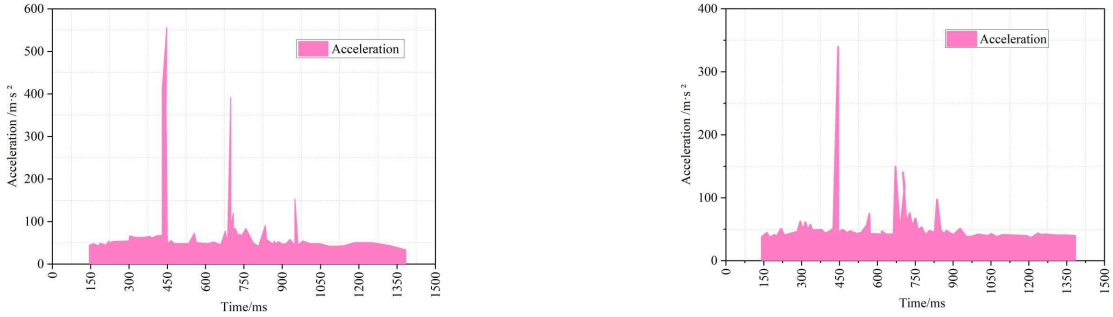

(a) Head acceleration situation (b) Chest acceleration situation

Figure 6: The force conditions causing injury at different time periods

IV. Conclusion

This paper integrates parallelized UAV 3D reconstruction technology and virtual reality technology to construct a multi-scene analysis and simulation system for traffic accidents, and restore the accident scene conditions. The absolute error value is only 0.22 at the maximum and the relative error is in the range of 0.07%-0.43% through the accident scene images taken by the UAV. It is significantly lower than the maximum absolute error value of 5.30

and the relative error range of 2.11%-8.76% of the traditional ranging method. The 3D accident model is established by combining 4.5m+25m aerial height images, and the relative errors are only 0.125 and 0.250 in the x-direction and y-direction, and the acceleration changes during the accident are calculated according to the accident model, which accurately restores the process of the three injuries of the driver. In the future, the lightweight algorithm can be further introduced to accelerate the speed of accident modeling and improve the ability of the simulation system to simultaneously restore multiple accident scenes.

Funding

This work was supported by Special Fund for Education and Scientific Research of Fujian Province.

References

[1] Mohammed, S. I. (2023). An overview of traffic accident investigation using different techniques. Automotive experiences, 6(1), 68-79.
[2] Huang, X., He, P., Rangarajan, A., & Ranka, S. (2020). Intelligent intersection: Two-stream convolutional networks for real-time near-accident detection in traffic video. ACM Transactions on Spatial Algorithms and Systems (TSAS), 6(2), 1-28.
[3] Wang, S., & Shang, Y. (2025). Pre-siting of UAV stations for traffic accident assessment considering road dispersion. PloS one, 20(2), e0316431.
[4] Liu, Z., Chen, C., Huang, Z., Chang, Y. C., Liu, L., & Pei, Q. (2024). A Low-Cost and Lightweight Real-Time Object-Detection Method Based on UAV Remote Sensing in Transportation Systems. Remote Sensing, 16(19), 3712.
[5] Dougald, L. E., Venkatanarayana, R., & Goodall, N. J. (2016). Traffic incident management quick clearance guidance and implications (No. FHWA/VTRC 16-R9, VTRC 16-R9). Virginia Transportation Research Council.
[6] Xu, Y., Hu, H., Huang, C., Nan, Y., Liu, Y., Wang, K., ... & Lian, S. (2024). TAD: A large-scale benchmark for traffic accidents detection from video surveillance. IEEE Access.
[7] Wang, Y., Zhang, Y., Piao, X., Liu, H., & Zhang, K. (2018). Traffic data reconstruction via adaptive spatial-temporal correlations. IEEE Transactions on Intelligent Transportation Systems, 20(4), 1531-1543.
[8] Zheng, J., Yang, Q., Liu, J., Li, L., Chai, Y., & Xu, P. (2023, January). Research on Road Traffic Accident Scene Investigation Technology Based on 3D Real Scene Reconstruction. In 2023 3rd Asia Conference on Information Engineering (ACIE) (pp. 38-43). IEEE.
[9] Kholodkov, K. I., Gukov, A. A., Scherbakov, V. M., Aleshin, I. M., & Gukov, A. A. (2024). 3D Reconstruction of an Accident Site. Izvestiya, Atmospheric and Oceanic Physics, 60(8), 963-969.
[10] Duma, I., Burnete, N., & Todorut, A. (2022). A review of road traffic accidents reconstruction methods and their limitations with respect to the national legal frameworks. In IOP Conference Series: Materials Science and Engineering (Vol. 1220, No. 1, p. 012055). IOP Publishing.
[11] Qu, A., & Wu, C. (2025). Revisiting the correlation between simulated and field-observed conflicts using large-scale traffic reconstruction. Accident Analysis & Prevention, 210, 107808.
[12] Chen, Y., Zhang, Q., & Yu, F. (2025). Transforming traffic accident investigations: a virtual-real-fusion framework for intelligent 3D traffic accident reconstruction. Complex & Intelligent Systems, 11(1), 76.
[13] Cujó Blasco, J., Bemposta Rosende, S., & Sánchez-Soriano, J. (2023). Automatic Real-Time Creation of Three-Dimensional (3D) Representations of Objects, Buildings, or Scenarios Using Drones and Artificial Intelligence Techniques. Drones, 7(8), 516.
[14] Cheng, M. L., Matsuoka, M., Liu, W., & Yamazaki, F. (2022). Near-real-time gradually expanding 3D land surface reconstruction in disaster areas by sequential drone imagery. Automation in Construction, 135, 104105.
[15] Gohari, A., Ahmad, A. B., Rahim, R. B. A., Elamin, N. I. M., Gismalla, M. S. M., Oluwatosin, O. O., ... & Lawal, A. (2023). Drones for road accident management: A systematic review. IEEE Access, 11, 109247-109256.
[16] Zulkifli, M. H., & Tahar, K. N. (2023). The Influence of UAV Altitudes and Flight Techniques in 3D Reconstruction Mapping. Drones, 7(4), 227.
[17] Stuchlík, R., & Kubíček, P. (2021). Fast and High Precise Spatial Documentation of Traffic Accident Site Using Only Low-Cost RPAS. Applied Sciences, 11(9), 4013.
[18] Pádua, L., Sousa, J., Vanko, J., Hruška, J., Adão, T., Peres, E., ... & Sousa, J. J. (2020). Digital reconstitution of road traffic accidents: A flexible methodology relying on UAV surveying and complementary strategies to support multiple scenarios. International journal of environmental research and public health, 17(6), 1868.
[19] Pérez, J. A., Gonçalves, G. R., Barragan, J. R. M., Ortega, P. F., & Palomo, A. A. M. C. (2024). Low-cost tools for virtual reconstruction of traffic accident scenarios. Heliyon, 10(9).
[20] Perc, M. N., & Topolšek, D. (2020). Using the scanners and drone for comparison of point cloud accuracy at traffic accident analysis. Accident Analysis & Prevention, 135, 105391.
[21] Zhang, X., Guan, Z., Liu, X., & Zhang, Z. (2025). Digital Reconstruction Method for Low-Illumination Road Traffic Accident Scenes Using UAV and Auxiliary Equipment. World Electric Vehicle Journal, 16(3), 171.
[22] Amin, M., Abdullah, S., Abdul Mukti, S. N., Mohd Zaidi, M. H. A., & Tahar, K. N. (2020). Reconstruction of 3D accident scene from multirotor UAV platform. The International Archives of the Photogrammetry, Remote Sensing and Spatial Information Sciences, 43, 451-458.
[23] Chidburee, P., Sriphannam, S., & Waisurasingha, C. (2022). Toward 3D reconstruction of damaged vehicles for investigating traffic accidents in Thailand using a photogrammetric approach. Engineering and applied science research, 49(4), 485-494.
[24] Vida, G., Melegh, G., Süveges, Á., Wenszky, N., & Török, Á. (2023). Analysis of UAV flight patterns for road accident site investigation. Vehicles, 5(4), 1707-1726.
[25] Saveliev, A., Lebedeva, V., Lebedev, I., & Uzdiaev, M. (2022). An approach to the automatic construction of a road accident scheme using UAV and deep learning methods. Sensors, 22(13), 4728.